

Bright sink-type localized states in exciton-polariton condensates

Michał Kulczykowski, Nataliya Bobrovska, and Michał Matuszewski

Institute of Physics, Polish Academy of Sciences, Aleja Lotników 32/46, 02-668 Warsaw, Poland

(Received 16 January 2015; revised manuscript received 3 June 2015; published 25 June 2015)

The family of one-dimensional localized solutions to dissipative nonlinear equations includes a variety of objects such as sources, sinks, shocks (kinks), and pulses. These states are in general accompanied by nontrivial density currents, which are not necessarily related to the movement of the object itself. We investigate the existence and physical properties of sink-type solutions in nonresonantly pumped exciton-polariton condensates modeled by an open-dissipative Gross-Pitaevskii equation. While sinks possess density profiles similar to bright solitons, they are qualitatively different objects as they exist in the case of repulsive interactions and represent a heteroclinic solution. We show that sinks can be created in realistic systems with appropriately designed pumping profiles. We also consider the possibility of creating sinks in a two-dimensional configuration with a ring-shaped pumping profile.

DOI: [10.1103/PhysRevB.91.245310](https://doi.org/10.1103/PhysRevB.91.245310)

PACS number(s): 71.36.+c, 03.75.Lm, 42.65.Tg, 78.67.—n

I. INTRODUCTION

Strong coupling of semiconductor excitons to microcavity photons results in the appearance of spectral resonances associated with mixed quantum quasiparticles called exciton polaritons [1]. These particles exhibit extremely light effective masses, few orders of magnitude smaller than the mass of electron, which allows for the observation of physical phenomena related to Bose-Einstein condensation already at room temperatures [2–9]. At the same time, polaritons exhibit strong exciton-mediated interparticle interactions and picosecond lifetime due to their photonic component. They are actively studied both from the point of view of fundamental interest [6–8] and potential applications [10,11].

In recent years, great attention has been devoted to the study of nonlinear self-localized states of superfluid polaritons, such as dark and bright solitons [12–17]. Solitons are nonlinear wave packets which preserve their shape thanks to the balance between dispersion and nonlinearity [18]. They have been applied to long-distance optical-fiber communication [19] as well as to the description of numerous physical systems. Polariton solitons have been demonstrated both in the cases of resonant [12,13] and nonresonant pumping [14–17]. To date, no bright states were shown to exist in the nonresonant case with homogeneous pumping.

Polariton superfluids are inherently nonequilibrium systems in which the balance between pumping and loss is an essential factor [2,9,20]. In many of the previous studies, this aspect was treated as an unwanted complication of the theory. Standard models, such as the conservative Gross-Pitaevskii equation, were frequently used to describe solitons. However, it is well known that self-localized solutions in dissipative systems have qualitatively different properties than their conservative counterparts. In the case of repulsive interactions, only one type of one-dimensional solution exists in the conservative theory—dark or bright solitons, depending on the sign of the effective mass. In the dissipative case, a family of qualitatively different localized states exists, including sources, sinks, shocks, and pulses [21–25]. In general, they exhibit nontrivial internal density currents and may undergo complicated, sometimes even chaotic, dynamics [15,26].

In this paper, we demonstrate the existence and stability of bright self-localized solutions of the open-dissipative polariton model. These solutions are classified as sinks (antidark solitons) [22,25], the name reflecting that their structure corresponds to terminating lines of incoming density currents, with a local increase of loss. While sink-type solutions possess density profiles similar to bright solitons, they are qualitatively different objects. In contrast to bright solitons, they exist in the case of repulsive interactions and represent a heteroclinic solution connecting two counterpropagating plane waves. We demonstrate the dynamics of sink formation and their stability in a realistic model with appropriately chosen pumping profile. We investigate systematically the properties of sinks and provide an approximate analytical formula for their shape. In the two-dimensional case, we show that sink creation is hindered by the spontaneous proliferation of vortices, which destroy the supercurrents necessary for the existence of a symmetric sink solution.

II. MODEL

We consider a polariton condensate in the one-dimensional (1D) setting, e.g., trapped in a microwire [27]. We model the system with the generalized open-dissipative Gross-Pitaevskii equation for the condensate wave function $\psi(x,t)$ coupled to the rate equation for the polariton reservoir density, $n_R(x,t)$ [15,20,28],

$$\begin{aligned}
 i\hbar\frac{\partial\psi}{\partial t} &= -\frac{\hbar^2 D}{2m^*}\frac{\partial^2\psi}{\partial x^2} + g_C^{1D}|\psi|^2\psi + g_R^{1D}n_R\psi \\
 &\quad + i\frac{\hbar}{2}(R^{1D}n_R - \gamma_C)\psi, \\
 \frac{\partial n_R}{\partial t} &= P(x) - (\gamma_R + R^{1D}|\psi|^2)n_R, \tag{1}
 \end{aligned}$$

where $P(x)$ is the exciton creation rate determined by the pumping profile, m^* is the effective mass of lower polaritons, γ_C and γ_R are the polariton and exciton loss rates, and $(R^{1D}, g_i^{1D}) = (R^{2D}, g_i^{2D})/\sqrt{2\pi d^2}$ are the rates of stimulated scattering into the condensate and the interaction coefficients, rescaled in the one-dimensional case. Here, we assumed a Gaussian transverse profile of $|\psi|^2$ and n_R of width d . In the

case of a one-dimensional microwire [27], the profile width d is of the order of the microwire thickness. We also introduced $D = 1 - iA$, with A being a small constant accounting for the energy relaxation in the condensate [27–30].

To obtain a system of dimensionless evolution equations, it is possible to rescale time, space, wave-function amplitude, and material coefficients according to $t = \tau \tilde{t}$, $x = \xi \tilde{x}$, $\psi = (\xi\beta)^{-1/2} \tilde{\psi}$, $n_R = (\xi\beta)^{-1} \tilde{n}_R$, $R^{1D} = (\xi\beta/\tau) \tilde{R}$, $(g_C^{1D}, g_R^{1D}) = (\hbar\xi\beta/\tau)(\tilde{g}_C, \tilde{g}_R)$, $(\gamma_C, \gamma_R) = \tau^{-1}(\tilde{\gamma}_C, \tilde{\gamma}_R)$, and $P(x) = (1/\xi\beta\tau) \tilde{P}(x)$, where $\xi = \sqrt{\hbar\tau/2m^*}$, while τ and β are arbitrary scaling parameters. We rewrite the above equation in the dimensionless form (we omit the tildes for convenience),

$$i \frac{\partial \psi}{\partial t} = \left[-D \frac{\partial^2}{\partial x^2} + g_C |\psi|^2 + g_R n_R + \frac{i}{2} (R n_R - \gamma_C) \right] \psi, \quad (2)$$

$$\frac{\partial n_R}{\partial t} = P(x) - (\gamma_R + R |\psi|^2) n_R.$$

In the above transformations the norms of both fields $N_\psi = \int |\psi|^2 dx$ and $N_R = \int n_R dx$ are multiplied by the factor of β .

III. SINK-TYPE SOLUTIONS

A. Description of sink solutions

The structure of sink solutions can be understood most easily as a result of the interaction of two counterpropagating nonlinear waves. In the linear case, two waves emitted by distant sources give rise to a standard interference pattern, as shown in Fig. 1(a). In the case of a dissipative model with nonlinear gain or loss coefficients, the interference pattern can be replaced by a localized density peak, sometimes exhibiting oscillating features, as depicted in Fig. 1(b). Sink is a heteroclinic solution connecting two plane waves emitted by the sources at each side. The two waves collide at the sink position, where the incoming density currents are dissipated [22].

The sink density pattern is a result of the ability of the dissipative medium to smooth out density “dips” and “peaks,” which are present in the standard interference pattern. When

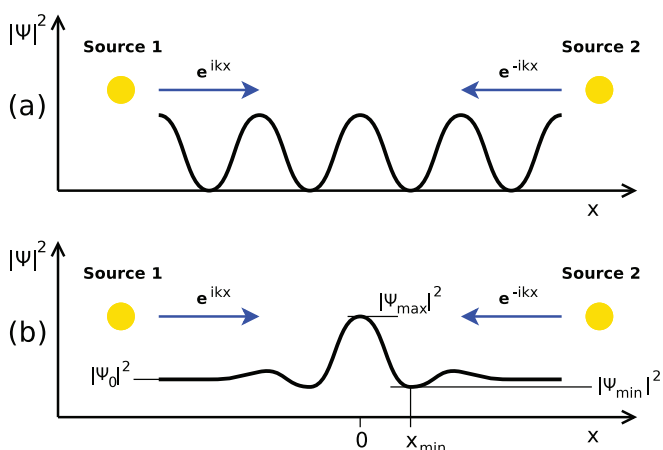


FIG. 1. (Color online) Density patterns created with counterpropagating waves. (a) Interference pattern in the linear regime. (b) Stationary sink-type localized pattern in a model with nonlinear dissipation.

one of the incoming waves reaches the area occupied by the other, the resulting interference leads to decay of waves. Let us consider one of the simplest dissipative nonlinear wave equations, the complex Ginzburg-Landau equation [22,23] (CGLE),

$$\frac{\partial \psi}{\partial t} = \left[iD \frac{\partial^2}{\partial x^2} + iC |\psi|^2 - iB \right] \psi. \quad (3)$$

This equation can be obtained from the system of equations (2) in the limit of fast relaxation time of the reservoir, which is “slaved” by the slower ψ dynamics, and in the linearized approximation $|\psi|^2 \approx n_0 \equiv \text{Im}B/\text{Im}C = (P - P_{\text{th}})/\gamma_C$ (n_0 is the dynamical equilibrium density when the loss and gain are balanced). Here, we assumed a homogeneous pumping $P(x) = \text{const} > P_{\text{th}}$ and introduced the threshold power $P_{\text{th}} = \gamma_R \gamma_C / R$. The CGLE parameters are $B = i\gamma_C/2 - (g_R + iR/2)(1 + Rn_0/\gamma_A)P/\gamma_A$ and $C = (g_R + iR/2)PR/\gamma_A^2 - g_C$ with $\gamma_A = Rn_0 + \gamma_R$. It is clear that the existence and stability of the homogeneous steady state with $n_0 > 0$ (which, in general, can also be a plane-wave solution) requires $\text{Im}B > 0$ and $\text{Im}C > 0$. Under these conditions, perturbations of the steady state with density n_0 exponentially decay, which is the reason for the above-mentioned smoothing. Any areas of density higher than n_0 correspond to net loss, and those with density lower than n_0 correspond to net gain in Eq. (3). Nevertheless, nontrivial (non-plane-wave) stationary solutions can still exist [15,22,23].

One can formulate another necessary condition for stability of sinks based on the modulational (or Benjamin-Feir) stability of the incoming plane waves [22]. In the case of CGLE with real $D > 0$, this is assured by the condition $\text{Re}C < 0$, which in terms of Eq. (2) translates into $P/P_{\text{th}} > (\gamma_C g_R / \gamma_R g_C)$, as shown recently in [17]. We note that this is a necessary condition for stability, and an actual domain of stability of plane waves may be smaller [28].

It may seem natural to treat sinks as dissipative analogues of bright solitons. These states are, however, qualitatively different from each other. Bright solitons exist in the conservative limit of the CGLE (3) with $\text{Im}(C, B, D) = 0$, which is the celebrated nonlinear Schrödinger equation [31] (or Gross-Pitaevskii equation in the context of degenerate bosons [32]). Sinks require nonzero incoming currents for their existence [22] and exist in the case of a stable background, $\text{Re}(CD) < 0$, while bright solitons exist only in the self-focusing (modulationally unstable) case with $CD > 0$.

B. Sinks in the exciton-polariton model

To create sink solutions in the model described by (2), one has to provide sources of counterpropagating waves as described above. We consider the following pumping profile created by a pumping beam with spatially varying intensity:

$$P(x) = P_{\max} e^{-(x/w_b)^\alpha} - (P_{\max} - P_0) e^{-(x/w_s)^\beta}, \quad (4)$$

as shown in Fig. 2 (dashed lines), where we used the smoothness parameters $\alpha = 100$ and $\beta = 80$. The profile exhibits jumps of $P(x)$ at $x = \pm w_b$ and $x = \pm w_s$, typical of the super-Gaussian terms in (4).

The sink is created in the central area with pumping intensity $P = P_0$. The side areas with $P = P_{\max}$ are the

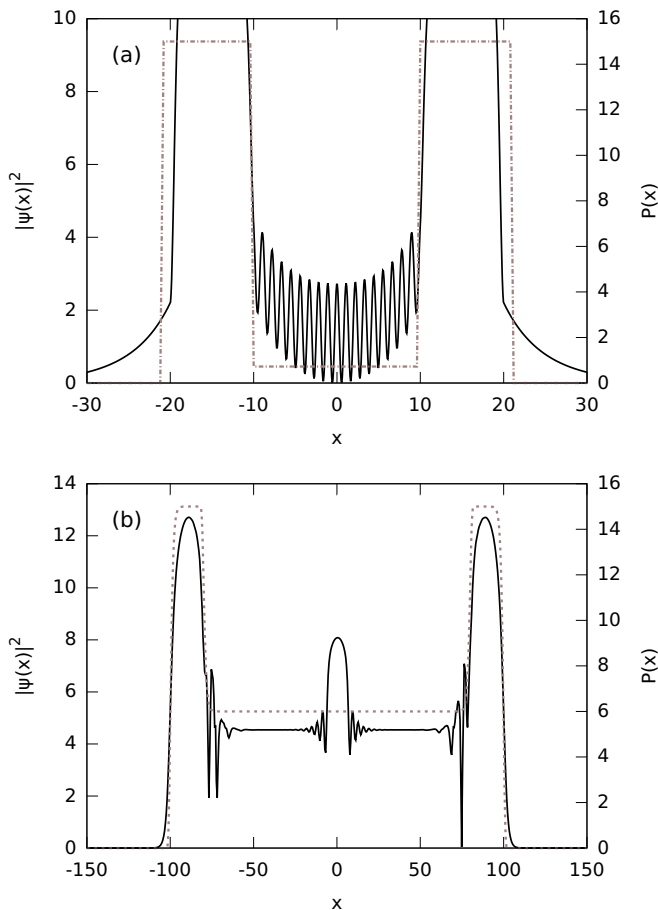


FIG. 2. (Color online) Patterns created by polariton waves emitted by high-intensity sources on the two sides with pumping profiles as in (4) (dashed lines). (a) A stationary interference pattern obtained by integration of (2) in time for parameters $A = 0.1$, $R = 0.96$, $g_C = 0.63$, $g_R = 1.91$, $\gamma_C = 0.9$, and $\gamma_R = 0.6$ at low pumping powers. (b) With a stronger pumping P_0 , a nonlinear sink-type solution is created. Corresponding parameters in physical units are time unit $\tau = \gamma_C^{-1} = 3$ ps, length unit $\xi = 1.9 \mu\text{m}$, $g = 3.9 \mu\text{eV}\mu\text{m}^2$, $R = 9 \times 10^{-3} \mu\text{m}^2 \text{ps}^{-1}$ for $d = 2 \mu\text{m}$, $m^* = 5 \times 10^{-5} m_e$, and $\beta = 0.003$.

sources of polariton waves. This flow is obtained thanks to the repulsive polariton-polariton and reservoir-polariton interactions $g_C, g_R > 0$, which create an effective potential hill in the areas with high pumping density, $P = P_{\text{max}}$. As a result of the interaction of the two nonlinear waves propagating towards the center, depending on the parameters of the system, interference or localized sink patterns can appear, as shown in Figs. 2(a) and 2(b), respectively. Note that at the interface between the high- and low-pumping areas at $x = \pm w_s$ in Fig. 2(b), oscillating time-dependent states form, which do not, however, preclude the formation of sinks. We also obtained different, more complicated nonlinear patterns for other values of parameters, especially in the case when the two sources were relatively close to each other. These patterns did not have a localized character such as the one shown in Fig. 2(b). A small value of relaxation coefficient $A = 0.1$ was in some cases necessary to attenuate high-momentum modes in simulations and obtain physically relevant solutions.

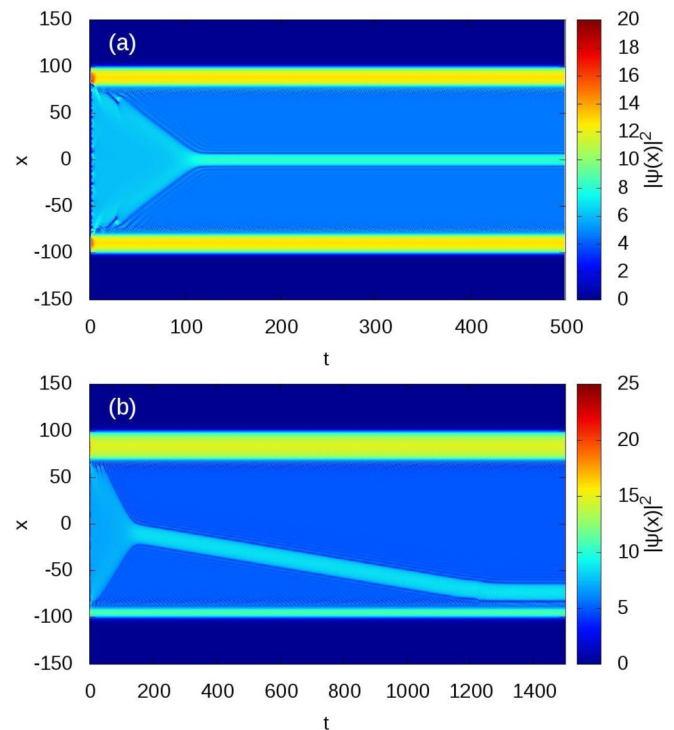


FIG. 3. (Color online) (a) Evolution towards a stationary sink state from a small initial noise. Parameters are as in Fig. 2(b). (b) The case of asymmetric pumping profile, with momentum mismatch between the waves from the two sources. The sink moves towards the weaker source, where it is stopped but not destroyed.

Figure 3(a) shows the dynamics of the sink-creation process. Initially, we assumed zero density of excitons and a small white noise in the polariton field, but we checked that the final stationary state is practically independent of the form of the initial condition. First, in the area between the sources, a condensate is created with approximately zero momentum. The wave fronts generated by the sources gradually move towards the center, where they collide creating the stable sink structure. The waves are “stopped” by the sink due to the nonlinear character of the gain and dissipation.

It is important to note that the sinks are, in general, not completely stationary, as in Fig. 3(a), but may be put in motion by the imbalance of momenta of the waves emitted by the two sources; see Fig. 3(b). In this case, the sink moves with a constant velocity proportional to the mismatch between the two wave vectors [22]. This behavior is qualitatively different from that of CGLE solitons pinned by localized gain [33]. If the balance is restored after some period of time, the sink stops at the new position. The sink may also be stopped after reaching the weaker source, as demonstrated in Fig. 3(b).

IV. DOMAIN OF EXISTENCE AND PROPERTIES OF SINKS

In this section, we describe a systematic investigation of stationary sink solutions of the exciton-polariton model with homogeneous pumping, $P(x) = \text{const}$. We substitute $\psi(x, t) = \phi(x)e^{-i\mu t}$ and $n_R(x, t) = n_R(x)$ into Eqs. (2) to obtain a single ordinary differential equation for the profile

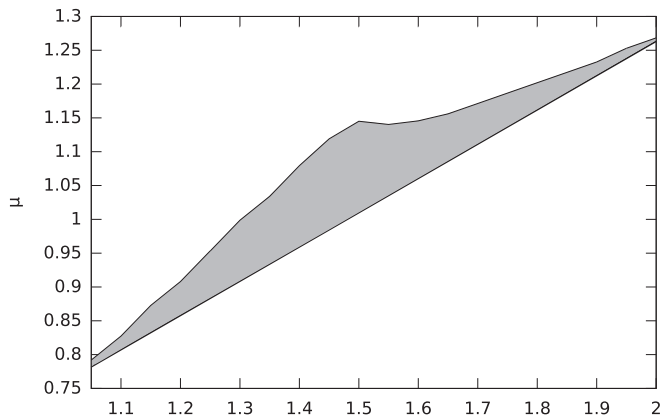


FIG. 4. Phase diagram depicting parameters for which a sink solution was obtained with (5) (gray area). Parameters are $R = 0.76, g_C = 0.38, g_R = 0.76, \gamma_C = 0.75, \gamma_R = 1$.

of the stationary state,

$$\begin{aligned} \frac{d^2\phi}{dx^2} = & -\mu\phi + g_C|\phi|^2\phi + g_R \frac{P}{\gamma_R + R|\phi|^2}\phi \\ & + \frac{i}{2} \frac{RP}{\gamma_R + R|\phi|^2}\phi - \frac{i}{2}\gamma_C\phi. \end{aligned} \quad (5)$$

We complement the above equation with boundary conditions. At $x = 0$, which we chose to be the symmetry point without loss of generality, the first derivative is equal to zero, $d\phi/dx = 0$. At $x = +\infty$, the solution tends to the plane wave with the norm equal to $|\phi|^2 = n_0 = (P - P_{th})/\gamma_C$ (in practice, we impose this condition on the last point of the computational mesh).

We solve the boundary problem with the shooting method using the Newton minimization algorithm. We keep $\frac{d\phi}{dx}|_{x=0} = 0$ and change the value of $\phi(0)$ while solving (5) with the Runge-Kutta algorithm on a certain interval, $0 < x < x_{max}$. The Newton method is then used to find a solution that satisfies boundary condition $|\phi|^2 = n_0$ at $x = x_{max}$ within a given tolerance. We then extend the interval boundary x_{max} slightly and repeat our procedure. This method proved to be an effective way to obtain a localized state on a large- x domain.

Figure 4 presents a phase diagram showing the domain of existence of sink-type solutions in the parameter space of P and μ with values of other parameters fixed. The shaded area, corresponding to parameters for which the algorithm converged to a sink solution, is limited from below by the natural minimum given by the chemical potential of the steady state,

$$\mu_{min} = g_C n_0^2 + \frac{P g_R}{(\gamma_R + R n_0^2)}. \quad (6)$$

The range of μ for which the sink solution exists turned out to be the largest for moderate pumping intensities, $P \approx 1.5 P_{th}$. Although the range of μ appears to be small, it corresponds in fact to a broad range of wave numbers of incoming waves, from approximately zero to around six, as shown in Fig. 5(a) with a dash-dotted line. In this figure, the vertical line corresponds to the minimal value of μ , given by Eq. (6). The dependence between the chemical potential and the wave

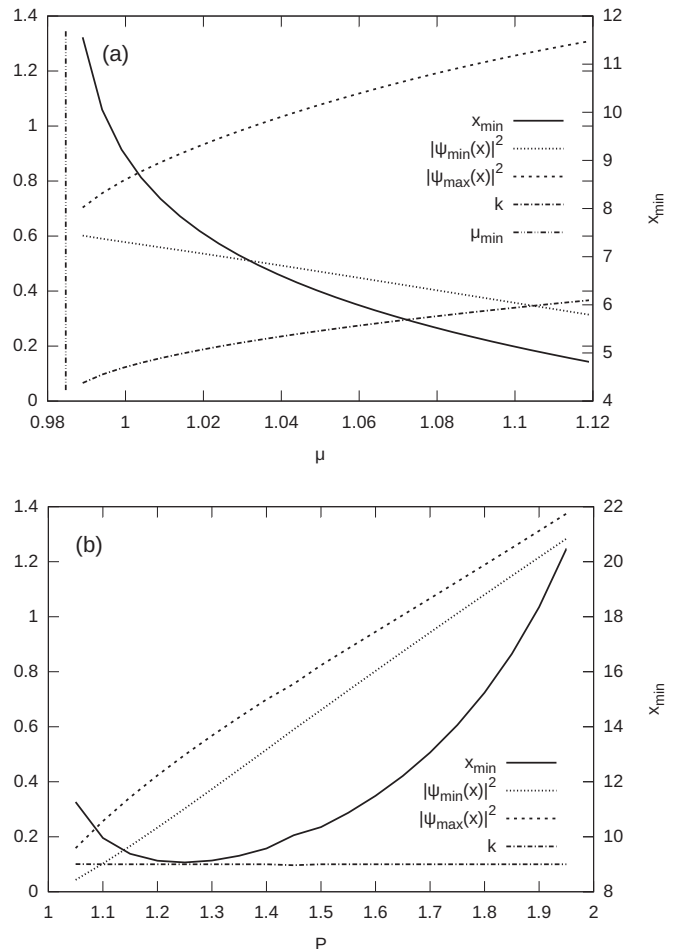


FIG. 5. The values of $|\psi_{min}(x)|^2$, $|\psi_{max}(x)|^2$, x_1 and the wave vector k (see Fig. 1 for descriptions). (a) We keep a constant value of $P = 1.45$ but vary the chemical potential μ . The value of x_{min} quickly decreases, indicating that at higher μ , the sink is more densely undulating. The dependence of $|\psi_{min}(x)|^2$ and $|\psi_{max}(x)|^2$ shows that the sink “height” is increased at higher μ . (b) We change the value of P while μ is chosen slightly higher than the lower threshold μ_{min} for which a sink solution occurs. The dependence of $|\psi_{min}(x)|^2$, $|\psi_{max}(x)|^2$ on P indicates that sink height is approximately constant while the background density n_0 grows with P .

number of incoming waves can be calculated by taking the $x \rightarrow \pm\infty$ limit away from the sink, for which Eq. (5) reduces to $\mu = k^2 + g_C n_0^2 + P g_R / (\gamma_R + R n_0^2)$ under the condition of balanced gain and loss. It is then clear that the necessary condition for the existence of sinks is that the kinetic energy is much smaller than the nonlinear energy of the wave.

The dashed and dotted lines in Fig. 5(a) depict the minimum and maximum density of the sink profile; see Fig. 1. With increasing μ , which corresponds to increasing k vectors of incoming waves, the sinks become larger and more highly modulated, while in the $\mu = \mu_{min}$ limit, they transform smoothly to the flat homogeneous state $\phi(x,t) = n_0 e^{-i\mu_{min}t}$. The position of the first minimum of the density x_{min} (solid line) decreases with the increase of μ , which is related to the increasingly dense interference pattern of the tails of the sink.

Figure 5(b) shows the dependence of the same properties of the sink as described above, but with increasing pumping power P . Here, μ is kept at a slightly increased level with respect to μ_{\min} . This corresponds to a constant small value of k . In this case, the increase of P leads to the increase of average sink density, but without almost any change of the difference $|\phi_{\max}|^2 - |\phi_{\min}|^2$. On the other hand, the value of x_{\min} shows a strongly nonmonotonous character, decreasing for small P and increasing again for large P . This shows that in the case of small k , the position of first minimum is not simply related to the incoming wave vector k .

V. ANALYTICAL SOLUTION

If the “height” of the sink is relatively small compared to the steady-state density, $|\psi(x,t) - n_0| \ll n_0$, and the amplitude $|\psi(x,t)|$ is slowly varying in space, an approximate analytical solution can be found [34]. We rewrite the steady-state solution in a homogeneously pumped condensate applying the Madelung transformation for $\psi(x,t)$,

$$\psi(x,t) = a(x)e^{i(\varphi(x) - \mu t)}, \quad n_R(x,t) = n_R(x), \quad (7)$$

where $a(x)$ is the amplitude, $\varphi(x)$ is the phase, and μ is the chemical potential of the condensate. Neglecting the spatial derivatives of $a(x)$, Eq. (2) can be rewritten as

$$i\mu = i \left\{ ga^2(x) + g_R n_R(x) + \left[\frac{d}{dx} \varphi(x) \right]^2 \right\} - \left\{ \frac{1}{2} [Rn_R(x) - \gamma_C] - \frac{d^2}{dx^2} \varphi(x) \right\}. \quad (8)$$

The real part of Eq. (8), which can be interpreted as the continuity equation, gives

$$n_R(x) = \frac{2}{R} \left[\frac{d^2}{dx^2} \varphi(x) \right] + \frac{\gamma_C}{R}. \quad (9)$$

On the other hand, solving the equation for reservoir density (2) in the steady state, we get

$$n_R(x) = \frac{P}{a^2(x)R + \gamma_R}. \quad (10)$$

We expand this formula into Taylor series of degree two around $a^2(x) = n_0 = (P/\gamma_C) - (\gamma_R/R)$,

$$n_R(x) = -\frac{\gamma_C [a^2(x)R\gamma_C - 2PR + \gamma_C\gamma_R]}{PR^2}. \quad (11)$$

Comparing Eqs. (9) and (11), we obtain

$$a^2(x) = -\frac{2PR \left[\frac{d^2}{dx^2} \varphi(x) \right] - PR\gamma_C + \gamma_C\gamma_R}{R\gamma_C^2}. \quad (12)$$

From the imaginary part of Eq. (8), using (9) and (12) we get

$$\mu = -\frac{g}{R\gamma_C^2} \left\{ 2PR \left[\frac{d^2}{dx^2} \varphi(x) \right] - PR\gamma_C + \gamma_C^2\gamma_R \right\} + g_R \left\{ \frac{2}{R} \left[\frac{d^2}{dx^2} \varphi(x) \right] + \frac{\gamma_C}{R} \right\} + \left[\frac{d}{dx} \varphi(x) \right]^2. \quad (13)$$

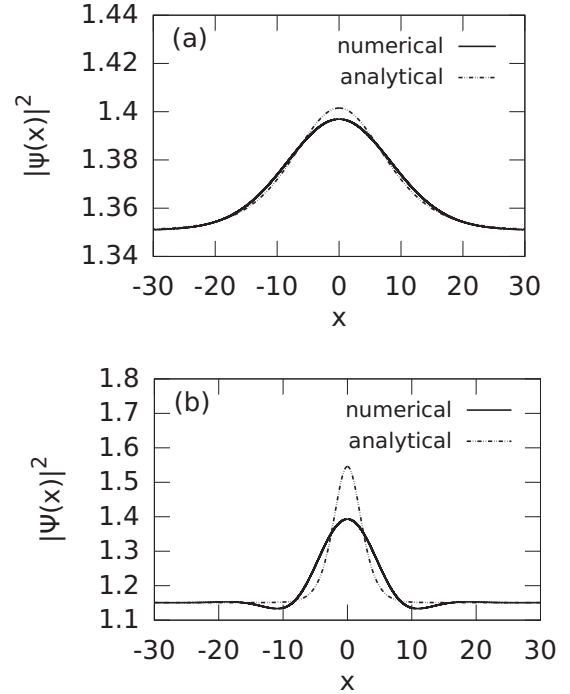


FIG. 6. Comparison of the numerical sink solution from the shooting method with the approximate analytical solution for two sets of parameters. Parameters are (a) $R = 0.76$, $g = 0.38$, $g_R = 2g$, $\gamma_C = 0.75$, $\gamma_R = 1$, $P = 2.0$, $\mu = 1.2683$ and (b) $P = 1.85$, $\mu = 1.2173$.

With the definition $\xi(x) = \frac{d}{dx} \varphi(x)$, we obtain the first-order differential equation

$$2 \left(\frac{g_R}{R} - \frac{gP}{\gamma_C^2} \right) \frac{d}{dx} \xi(x) + \xi^2(x) + \left[g \left(\frac{P}{\gamma_C} - \frac{\gamma_R}{R} \right) + \frac{g_R\gamma_C}{R} - \mu \right] = 0, \quad (14)$$

with the solution

$$\xi(x) = \frac{\sqrt{\delta}}{R\gamma_C} \tan \left(\frac{1}{2} \frac{\sqrt{\delta}}{\alpha} x \right), \quad (15)$$

where $\delta = R(PRg\gamma_C - R\mu\gamma_C - g\gamma_C^2\gamma_R + g_R\gamma_C^3)$ and $\alpha = gPR - g_R\gamma_C^2$. Calculating the amplitude with (12), we finally obtain

$$a^2(x) = -\frac{1}{R\gamma_C^2} \left\{ \frac{\delta P}{\alpha} \left[1 + \tan^2 \left(\frac{1}{2} \frac{\gamma_C \sqrt{\delta}}{\alpha} x \right) \right] - PR\gamma_C + \gamma_C^2\gamma_R \right\}. \quad (16)$$

A comparison between the analytical and numerical solution obtained with the shooting method is shown in Fig. 6. In general, very good agreement is obtained for small k , when the sink profile is flat and broad, with no oscillating tails. The tails obviously cannot be reproduced by the approximate solution (16), which is visible in Fig. 6(b).

VI. TWO-DIMENSIONAL CASE

Additionally, we performed a series of simulations to investigate whether sink creation is possible in the

two-dimensional (2D) version of the exciton-polariton model, described by the equations

$$i \frac{\partial \psi}{\partial t} = \left[-D \left(\frac{\partial^2}{\partial x^2} + \frac{\partial^2}{\partial y^2} \right) + g_C |\psi|^2 + g_R n_R + \frac{i}{2} (R n_R - \gamma_C) \right] \psi, \quad (17)$$

$$\frac{\partial n_R}{\partial t} = P(x, y) - (\gamma_R + R |\psi|^2) n_R, \quad (18)$$

where $g_{R,C}$, $\gamma_{R,C}$, R , and $P(x, y)$ are dimensionless parameters obtained from physical ones in an analogous way as in the 1D case.

One of the possible choices of the pumping profile corresponds to a constant $P = P_0$ pumping intensity on a circle of radius r_1 , surrounded by a ring of $P = P_{\max}$ with inner and outer radius r_1 and r_2 , respectively. In Fig. 7, we show a typical state obtained with this kind of pumping profile and an evolution from a small initial noise. In general, after a certain time of evolution, a smaller or larger number of vortices is spontaneously created, and often a stationary state could never be reached even with a very long integration time. Vortices may appear spontaneously during condensation in a process analogous to the Kibble-Zurek mechanism [35–37], as well as due to the emergence of supercurrents in an inhomogeneous system [7,38]. Despite the use of various combinations of system parameters, as well as asymmetric ring pumping profiles, we were not able to obtain any stable structures that would resemble one-dimensional sinks of the previous sections.

We note that similar pumping profiles were used in several experiments [39,40] where multilobe or vortex patterns were observed. However, the experimental patterns were in most cases regular, which suggests that they correspond to the linear regime as in Fig. 2(a). In the case of strong nonlinear interactions, regular vortex chain patterns could be observed with the resonant pumping scheme [39]. Depending on the system parameters, these could be destroyed by spontaneously nucleating vortices created through a hydrodynamic instability, which is consistent with our simulations.

VII. CONCLUSIONS

We demonstrated the existence and stability of a family of bright sink solutions of the open-dissipative polariton model. In contrast to bright solitons of conservative models, sinks exist in the case of repulsive interactions and are created in a collision of counterpropagating waves. We studied the dynamics of sink formation in a realistic one-dimensional

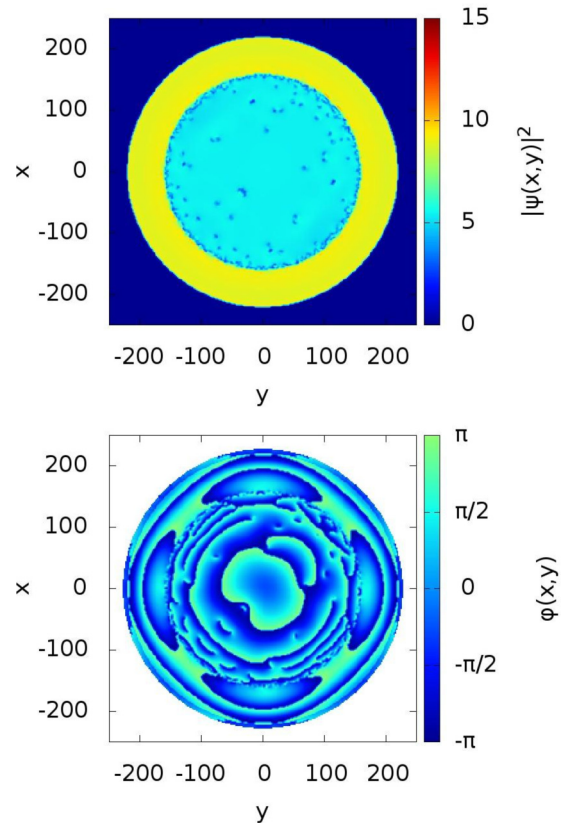


FIG. 7. (Color online) Snapshot of a two-dimensional solution of (18) after a long time of evolution, $t = 1600$, generated by a pumping profile in the shape of a ring. Quantum vortices are clearly visible in the density (top) and phase (bottom) of $\psi(x, y, t)$. Sink solutions in 2D are absent due to proliferation of vortices. Parameters are $A = 0.1$, $R = 0.96$, $g_C = 0.63$, $g_R = 1.91$, $\gamma_C = 1$, $\gamma_R = 0.6$ with $P_0 = 6$, $P_{\max} = 10$, $r_1 = 155$, $r_2 = 220$.

polariton model with appropriately chosen pumping profile. We studied the domain of existence of sinks in parameter space and their physical properties. An approximate analytical formula for the sink shape, valid in the case where sinks do not possess oscillating tails, was determined. In the two-dimensional ring-shaped configuration, sink solutions were not found due to the spontaneous appearance of vortices.

Note added. We note that recently bright soliton-like structures were observed in two-dimensional resonantly pumped polariton condensates [41], whose existence, however, could not be explained using the model (1).

ACKNOWLEDGMENT

We acknowledge support from the National Science Center Grant No. DEC-2011/01/D/ST3/00482.

[1] J. J. Hopfield, Phys. Rev. Lett. **112**, 1555 (1958); C. Weisbuch, M. Nishioka, A. Ishikawa, and Y. Arakawa, *ibid.* **69**, 3314 (1992); A. V. Kavokin, J. J. Baumberg, G. Malpuech, and F. P. Laussy, *Microcavities* (Oxford University Press, Oxford, 2007).

[2] J. Kasprzak, M. Richard, S. Kundermann, A. Baas, P. Jeambrun, J. M. J. Keeling, F. M. Marchetti, M. H. Szymańska, R. André, J. L. Staehli *et al.*, *Nature (London)* **443**, 409 (2006).

[3] S. Christopoulos, G. B. H. von Högersthal, A. J. D. Grundy, P. G. Lagoudakis, A. V. Kavokin, J. J. Baumberg, G. Christmann,

- R. Butté, E. Feltn, J.-F. Carlin *et al.*, *Phys. Rev. Lett.* **98**, 126405 (2007).
- [4] S. Kena-Cohen and S. R. Forrest, *Nat. Photon.* **4**, 371 (2010).
- [5] J. D. Plumhof, T. Stöferle, L. Mai, U. Scherf, and R. F. Mahrt, *Nat. Mater.* **13**, 247 (2014).
- [6] A. Amo, J. Lefrère, S. Pigeon, C. Adrados, C. Ciuti, I. Carusotto, R. Houdré, E. Giacobino, and A. Bramati, *Nat. Phys.* **5**, 805 (2009); G. Roumpos, M. Lohse, W. H. Nitsche, J. Keeling, M. H. Szymanska, P. B. Littlewood, A. Löffler, S. Hofling, L. Worschech, A. Forchel *et al.*, *Proc. Nat. Acad. Sci. USA* **109**, 6467 (2012).
- [7] K. G. Lagoudakis, M. Wouters, M. Richard, A. Baas, I. Carusotto, R. André, Le Si Dang, and B. Deveaud-Plédran, *Nat. Phys.* **4**, 706 (2008).
- [8] I. Carusotto and C. Ciuti, *Rev. Mod. Phys.* **85**, 299 (2013).
- [9] H. Deng, H. Haug, and Y. Yamamoto, *Rev. Mod. Phys.* **82**, 1489 (2010).
- [10] T. C. H. Liew, A. V. Kavokin, and I. A. Shelykh, *Phys. Rev. Lett.* **101**, 016402 (2008); C. Adrados, T. C. H. Liew, A. Amo, M. D. Martín, D. Sanvitto, C. Antón, E. Giacobino, A. Kavokin, A. Bramati, and L. Viña, *ibid.* **107**, 146402 (2011); D. Ballarini, M. de Giorgi, E. Cancellieri, R. Houdré, E. Giacobino, R. Cingolani, A. Bramati, G. Gigli, and D. Sanvitto, *Nat. Commun.* **4**, 1778 (2013); T. Gao, P. S. Eldridge, T. C. H. Liew, S. I. Tsintzos, G. Stavrinidis, G. Deligeorgis, Z. Hatzopoulos, and P. G. Savvidis, *Phys. Rev. B* **85**, 235102 (2012).
- [11] Ch. Schneider, A. Rahimi-Iman, N. Y. Kim, J. Fischer, I. G. Savenko, M. Amthor, M. Lerner, A. Wolf, L. Worschech, V. D. Kulakovskii *et al.*, *Nature (London)* **497**, 348 (2013); P. Bhattacharya, T. Frost, S. Deshpande, M. Z. Baten, A. Hazari, and A. Das, *Phys. Rev. Lett.* **112**, 236802 (2014).
- [12] A. Amo, S. Pigeon, D. Sanvitto, V. G. Sala, R. Hivet, I. Carusotto, F. Pisanello, G. Leménager, R. Houdré, E. Giacobino, C. Ciuti *et al.*, *Science* **332**, 1167 (2011); G. Grosso, G. Nardin, F. Morier-Genoud, Y. Léger, and B. Deveaud-Plédran, *Phys. Rev. B* **86**, 020509 (2012); R. Hivet, H. Flayac, D. D. Solnyshkov, D. Tanese, T. Boulier, D. Andreoli, E. Giacobino, J. Bloch, A. Bramati, G. Malpuech *et al.*, *Nat. Phys.* **8**, 724 (2012); A. V. Yulin, O. A. Egorov, F. Lederer, and D. V. Skryabin, *Phys. Rev. A* **78**, 061801 (2008).
- [13] M. Sich, D. N. Krizhanovskii, M. S. Skolnick, A. V. Gorbach, R. Hartley, D. V. Skryabin, E. A. Cerda-Méndez, K. Biermann, R. Hey, and P. V. Santos, *Nat. Photon.* **6**, 50 (2012); O. A. Egorov, D. V. Skryabin, A. V. Yulin, and F. Lederer, *Phys. Rev. Lett.* **102**, 153904 (2009); O. A. Egorov, A. V. Gorbach, F. Lederer, and D. V. Skryabin, *ibid.* **105**, 073903 (2010); O. A. Egorov, D. V. Skryabin, and F. Lederer, *Phys. Rev. B* **84**, 165305 (2011).
- [14] E. A. Ostrovskaya, J. Abdullaev, A. S. Desyatnikov, M. D. Fraser, and Y. S. Kivshar, *Phys. Rev. A* **86**, 013636 (2012); E. A. Ostrovskaya, J. Abdullaev, M. D. Fraser, A. S. Desyatnikov, and Y. S. Kivshar, *Phys. Rev. Lett.* **110**, 170407 (2013).
- [15] Y. Xue and M. Matuszewski, *Phys. Rev. Lett.* **112**, 216401 (2014).
- [16] F. PINSKER and H. Flayac, *Phys. Rev. Lett.* **112**, 140405 (2014); H. Terças, D. D. Solnyshkov, and G. Malpuech, *ibid.* **113**, 036403 (2014); **110**, 035303 (2013).
- [17] L. A. Smirnov, D. A. Smirnova, E. A. Ostrovskaya, and Y. S. Kivshar, *Phys. Rev. B* **89**, 235310 (2014).
- [18] E. Infeld and G. Rowlands, *Nonlinear Waves, Solitons and Chaos*, (Cambridge University Press, Cambridge, 2000).
- [19] A. Hasegawa and Y. Kodama, *Solitons in Optical Communications*, (Oxford University Press, Oxford, 1995).
- [20] M. Wouters and I. Carusotto, *Phys. Rev. Lett.* **99**, 140402 (2007).
- [21] B. A. Malomed, *Physica D* **8**, 353 (1983).
- [22] W. van Saarloos and P. C. Hohenberg, *Physica D* **56**, 303 (1992).
- [23] H. Sakaguchi, *Prog. Theor. Phys.* **89**, 1123 (1993); I. S. Aranson and L. Kramer, *Rev. Mod. Phys.* **74**, 99 (2002).
- [24] N. Bekki and K. Nozaki, *Phys. Lett. A* **110**, 133 (1985); R. Conte and M. Musette, in *Dissipative Solitons*, edited by N. Akhmediev and A. Ankiewicz, (Springer, New York, 2005).
- [25] L. Pastur, M.-T. Westra, and W. van de Water, *Physica D* **174**, 71 (2003); M. van Hecke, C. Storm, and W. van Saarloos, *ibid.* **134**, 1 (1999).
- [26] J. M. Soto-Crespo, N. Akhmediev, and A. Ankiewicz, *Phys. Rev. Lett.* **85**, 2937 (2000); N. Akhmediev, J. M. Soto-Crespo, and G. Town, *Phys. Rev. E* **63**, 056602 (2001).
- [27] E. Wertz, L. Ferrier, D. D. Solnyshkov, R. Johne, D. Sanvitto, A. Lemaître, I. Sagnes, R. Grousson, A. V. Kavokin, P. Senellart *et al.*, *Nat. Phys.* **6**, 860 (2010).
- [28] N. Bobrovskaya, E. A. Ostrovskaya, and M. Matuszewski, *Phys. Rev. B* **90**, 205304 (2014).
- [29] L. M. Sieberer, S. D. Huber, E. Altman, and S. Diehl, *Phys. Rev. Lett.* **110**, 195301 (2013).
- [30] D. Tanese, H. Flayac, D. Solnyshkov, A. Amo, A. Lemaître, E. Galopin, R. Braive, P. Senellart, I. Sagnes, G. Malpuech *et al.*, *Nat. Commun.* **4**, 1749 (2013).
- [31] C. Sulem and P.-L. Sulem, *The Nonlinear Schrödinger Equation* (Springer, Berlin, 1999).
- [32] C. J. Pethick and H. Smith, *Bose-Einstein Condensation in Dilute Gases* (Cambridge University Press, Cambridge, 2008).
- [33] B. A. Malomed, *J. Opt. Soc. Am. B* **31**, 2460 (2014).
- [34] O. Stiller, S. Popp, and L. Kramer, *Physica D* **84**, 424 (1995).
- [35] T. W. B. Kibble, *J. Phys. A* **9**, 1387 (1976); W. H. Żurek, *Nature (London)* **317**, 505 (1985).
- [36] K. G. Lagoudakis, F. Manni, B. Pietka, M. Wouters, T. C. H. Liew, V. Savona, A. V. Kavokin, R. André, and B. Deveaud-Plédran, *Phys. Rev. Lett.* **106**, 115301 (2011).
- [37] M. Matuszewski and E. Witkowska, *Phys. Rev. B* **89**, 155318 (2014).
- [38] J. Keeling and N. G. Berloff, *Phys. Rev. Lett.* **100**, 250401 (2008).
- [39] T. Boulier, H. Terças, D. D. Solnyshkov, Q. Glorieux, E. Giacobino, G. Malpuech, and A. Bramati, *Sci. Rep.* **5**, 9230 (2015).
- [40] F. Manni, K. G. Lagoudakis, T. C. H. Liew, R. André, and B. Deveaud-Plédran, *Phys. Rev. Lett.* **107**, 106401 (2011); A. Dreismann, P. Cristofolini, R. Balili, G. Christmann, F. PINSKER, N. G. Berloff, Z. Hatzopoulos, P. G. Savvidis, and J. J. Baumberg, *Proc. Natl. Acad. Sci. USA* **111**, 8770 (2014).
- [41] L. Dominici, M. Petrov, M. Matuszewski, D. Ballarini, M. De Giorgi, D. Colas, E. Cancellieri, B. Silva Fernández, A. Bramati, G. Gigli, A. Kavokin, F. Laussy, and D. Sanvitto, [arXiv:1309.3083](https://arxiv.org/abs/1309.3083).